Molecular Therapy
Methods & Clinical Development
Original Article

Adenovirus-Mediated LAMA3 Transduction Enhances Hemidesmosome Formation and Periodontal Reattachment during Wound Healing

Yongzheng Li,[1,5] Jing Zhang,[2,5] Zhenxuan Cheng,[4] Ying Wang,[3,5] Tingben Huang,[1,5] Kaichen Lai,[1,5] Xue Du,[1,5] Zhiwei Jiang,[1,5] and Guoli Yang[1,5]

[1]Department of Implantology, The Affiliated Stomatology Hospital, Zhejiang University School of Medicine, Hangzhou 310006, China; [2]Department of Prosthodontics, The Affiliated Stomatology Hospital, Zhejiang University School of Medicine, Hangzhou 310006, China; [3]Department of Endodontics, The Affiliated Stomatology Hospital, Zhejiang University School of Medicine, Hangzhou 310006, China; [4]Department of Oral Medicine, Zhejiang University School of Hospital, Hangzhou 310058, China; [5]Key Laboratory of Oral Biomedical Research of Zhejiang Province, Zhejiang University School of Stomatology, Hangzhou 310029, China

A robust dento-epithelial junction prevents external pathogenic factors from entering connective tissue and could be crucial for periodontal reattachment after periodontal surgery. The junctional epithelium (JE) is attached to the tooth surface through the hemidesmosome (HD) and internal basal lamina, where the primary component is laminin-332. Destruction of the JE leads to the loss of periodontal attachment. Traditional treatments are effective in eliminating local inflammation of the gingiva; however, few directly promote periodontal reattachment and HD formation. Here, we designed a gene-therapy strategy using the adenovirus-mediated human laminin-332 α3 chain (LAMA3) gene (Ad-LAMA3) transduced into a human-immortalized epidermal cell line (HaCaT) to study the formation of HD *in vitro*. Ad-LAMA3 promoted early adhesion and fast migration of HaCaT cells and increased expression of LAMA3 and type XVII collagen (BP180) significantly. Furthermore, HaCaT cells could facilitate formation of mature HDs after LAMA3 overexpression. *In vivo* experiments demonstrated that the JE transduced with Ad-LAMA3 could increase expression of LAMA3 and BP180 and "biological sealing" between the tooth and gingival epithelium. These results suggested that adenovirus-mediated LAMA3 transduction is a novel therapeutic strategy that promotes the stability and integration of the JE around the tooth during wound healing.

INTRODUCTION

Natural gingival connective tissue is connected firmly to the tooth surface through the nonkeratinized junctional epithelium (JE). The latter is necessary to form a "biological seal" and is the first barrier of periodontal tissue that can prevent invasion by foreign bodies from penetrating the underlying soft tissue.[1] Nevertheless, separation of the JE from the tooth surface can occur by clinical probing, intentional trauma, surgery using periodontal flaps, and periodontitis.[2] In 1985, Isidor et al.[3] described the "reunion" of gingival tissue and a tooth surface split by incision/injury as "periodontal reattachment" (PR). Therefore, the building of strong PR during wound healing plays a critical part in the maintenance of body defense.

Several traditional treatments (e.g., scaling, root planing) or antimicrobial agents (delivered systemically or locally) can promote reattachment of the JE and connective tissue.[4] Nevertheless, those therapies aim to remove dental plaque and calculus, eliminating inflammation. However, very little is known about the molecular mechanism of PR; few treatments that target PR directly or induce hemidesmosome (HD) formation are available.

The JE attaches to enamel through the internal basal lamina (IBL) and HDs.[5] One of the most important components of the IBL is laminin-332 (LM332).[6] LM332 is a heterotrimer consisting of α3, β3, and γ2 chains.[7] The α3 subunit of LM332 has a vital role in nucleation during HD assembly and in maintenance of the structural integrity of HDs.[8–11] Mutation or deletion of the LM332 α3 chain (LAMA3) can result in complete loss of LM332 in the basement membrane and affect HD formation, which eventually, can lead to junctional epidermolysis bullosa.[12,13] Taken together, those findings suggest that LAMA3 has a promising role in promoting LM332 synthesis and HD formation.

Previously, scholars have focused on improving epithelial biological sealing around implants and HD formation by coating titanium surfaces with LM332 or LM332-derived peptides.[14–18] However, exogenous LM332, as a macromolecular protein, can cause immune rejection in the body and rapid protein degradation. Furthermore, protein synthesis can be expensive and suboptimal for clinical application. Gene delivery has introduced new prospects for the overexpression of recombinant proteins. Several scholars have shown the promising effects of local transduction of genes for preventing bone loss and accelerating tooth movement.[19,20]

Received 19 May 2020; accepted 29 May 2020;
https://doi.org/10.1016/j.omtm.2020.06.001.

Correspondence: Guoli Yang, Key Laboratory of Oral Biomedical Research of Zhejiang Province, Zhejiang University School of Stomatology, The Affiliated Stomatology Hospital, Zhejiang University School of Medicine, Yan'an Road, Hangzhou 310006, China.
E-mail: guo_li1977@zju.edu.cn

Our previous study demonstrated that immobilization of recombinant adenovirus encoding LAMA3 on the implant surface via layer-by-layer assembly and antibody antigen-specific binding could promote the biological sealing of the peri-implant hard and soft tissues.[21] In the present study, we have investigated the effect of the adenovirus-mediated human LAMA3 gene (Ad-LAMA3) on PR via a direct injection approach. A model of JE injury in rats was induced, with or without direct injections of Ad-LAMA3, to ascertain the therapeutic utility of LAMA3 overexpression to improve binding between the JE and tooth surface *in vivo*. In this way, we wished to develop new treatment with firm and rapid biological sealing.

RESULTS

Optimization of Ad-LAMA3 Transduction Efficiency in HaCaT Cells

The low cytotoxicity and high transduction efficiency were used to determine the optimal multiplicity of infection (MOI). HaCaT cells (a human-immortalized epidermal cell line) were transduced with Ad-LAMA3 at an MOI of 110, 220, and 440 for 48 h. Expression of green fluorescent protein (GFP) showed that Ad-LAMA3 was successfully transduced into cells (Figure 1B). The transduction efficiency was >95% at an MOI of 220 and MOI of 440 (n = 3; Figure 1C). However, an MOI of 440 with the highest transduction efficiency could have cytotoxicity for the HaCaT growth (data not shown). Therefore, an MOI of 220 was selected as the optimal MOI for subsequent transduction experiments in this study.

Effects of the Ad-LAMA3 on the Proliferation, Adhesion, and Migration of HaCaT Cells

The alamarBlue assay was used to investigate the viability of HaCaT cells treated with Ad-LAMA3 or Ad-GFP after 1, 3, or 5 days. The number of HaCaT cells in the three groups showed no significant difference (n = 3; $p > 0.05$) (Figure 1D). These results suggested that transduction with Ad-LAMA3 or Ad-GFP did not inhibit proliferation of HaCaT cells.

The number of attached cells and cytoskeletal morphology were determined to investigate adhesion of HaCaT cells during early stages after treatment. From 3 h to 6 h after treatment with Ad-LAMA3 or Ad-GFP, the Ad-LAMA3 group showed significantly more attached cells than the other two groups (>1.4-fold increase; $p < 0.01$) (Figure 1E). The Ad-LAMA3 group exhibited more polygonal cells with pseudopodia, and simultaneously, most cells of the Ad-GFP group were small and circular (Figure 1G).

Scratch assays were used to assess the effect of Ad-LAMA3 on the migratory capacity of HaCaT cells. After 3 days of wound healing, compared with Ad-GFP treatment, HaCaT cells treated with Ad-LAMA3 showed a significant increase in %gap closure in scratch assays (1.5-fold increase; $p = 0.0093$). However, the migratory capacity of HaCaT cells in all groups showed no significant difference after 1 day of wound healing (Figure 1F). Figure 1H shows representative images of wound healing in the three groups at each time.

Effects of the Ad-LAMA3 on the Expression of HD-Related Genes and Proteins

Expression of HD-related genes was measured after cells had been treated with Ad-LAMA3 or Ad-GFP for 3 days or 5 days. mRNA expression of LAMA3 and type XVII collagen (BP180) in the Ad-LAMA3 group was significantly upregulated at each time point (Figures 2A and 2D). The expression level changes in the LAMA3 gene in the Ad-LAMA3 group were 4.6-fold and 1.7-fold higher at 3 and 5 days, respectively, compared with the Ad-GFP group. The mRNA levels of LAMB3 in the Ad-LAMA3 group were significantly higher than in the Ad-GFP group at 3 days ($p < 0.05$) (Figure 2B). Meanwhile, the expression levels of LAMC2 in the Ad-LAMA3 group were significantly higher than in the Ad-GFP group at 5 days ($p < 0.001$) (Figure 2C). Moreover, western blotting showed that expression of the HD-related proteins of LAMA3 and BP180 was upregulated significantly in the Ad-LAMA3 group, 5 days after transduction (Figures 2E–2G). The transduction effects of Ad-LAMA3 on HD-related genes and proteins revealed that LAMA3 overexpression could be beneficial to the anchorage of HD onto HaCaT cells *in vitro*.

Immunofluorescence Expression of LAMA3 and BP180 Proteins in HaCaT Cells

Immunofluorescence analyses showed that LAMA3 and BP180 exhibited red fluorescence, and nuclei showed blue fluorescence. LAMA3 proteins and BP180 proteins were distributed mainly in the cytoplasm and membrane of HaCaT cells (Figure 3). Moreover, BP180 protein was localized along the plasma membrane of the HD, a result that is in accordance with data from a study by Hiroyasu et al.[22] The immunoreactivity of these proteins in HaCaT cells treated with Ad-LAMA3 was stronger than that in the other groups. These results demonstrated that LAMA3 overexpression could contribute to HD formation.

Ad-LAMA3 Promotes HD Formation

To confirm further the results of immunofluorescence, we used transmission electron microscopy (TEM) to observe HD structures. HDs possess a tripartite, electron-dense, cytoplasmic plaque structure.[23] Hormia et al.[24] showed that HaCaT cells formed mature HDs after induction by 804G conditioned medium containing soluble laminin-5r. Nevertheless, HaCaT cells, cultured in conditioned medium, formed only primary HDs that lacked a sub-basal plate.[24] We observed a group of mature HDs in the Ad-LAMA3 group (Figure 4). However, the control group and Ad-GFP group had only rudimentary and immature HDs that lacked well-developed, tripartite, electron-dense plaques. These results suggested that Ad-LAMA3 treatment could promote the assembly of mature HDs.

Pathologic Morphology of the JE during Wound Healing

The JE of normal rats in the control group was located on the flank of the tooth surface of the gingival sulcus epithelium. The latter was discontinuous with the sulcus epithelium, irregular in shape, stained deeply, and thickened in the apical portion and often formed a fissure with the sulcus epithelium in the coronal portion. Moreover, the evident keratinized sulcular epithelium could be distinguished from

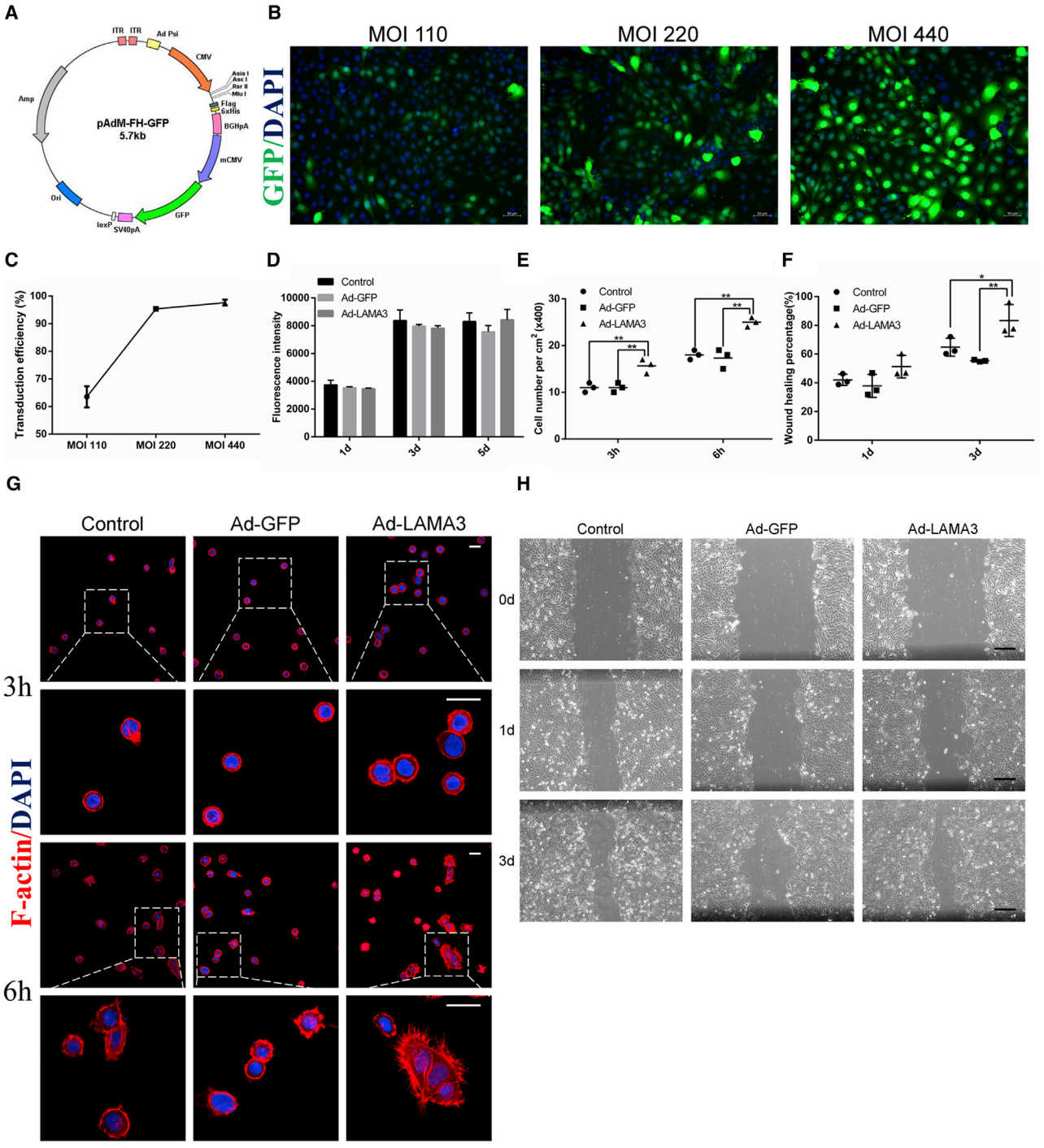

Figure 1. Effect of the Ad-LAMA3 on the Proliferation, Adhesion, and Migration of HaCaT Cells

(A) Adenovirus vector map. ITR, inverted terminal repeat; CMV, cytomegalovirus promoter; GFP, green fluorescent protein gene; Amp, ampicillin gene. (B) Representative images of GFP expression at an MOI of 110, 220, or 440 after 48 h. (C) Ad-LAMA3 transduction efficiency in HaCaT cells by counting the GFP-positive cells (n = 3 in each MOI). (D) Viability of HaCaT cells in different groups for 1, 3, or 5 days (n = 3 in each group). (E) Early adhesion assay of HaCaT cells cultured for 3 or 6 h. Cells were not treated (Control) or treated with Ad-GFP or Ad-LAMA3. Three randomly chosen fields in each sample were evaluated. (F) Percentage closure was calculated by measuring the wound width from images in each group. Bars represent the mean ± standard deviation for n = 3. *$p < 0.05$, **$p < 0.01$. (G) Representative images after 3 or 6 h of early adhesion. Scale bar, 25 μm. (H) Scratch assays on HaCaT cells treated with Ad-GFP or Ad-LAMA3. Representative images at the time of scratching (0 days) as well as 1 or 3 days after scratching. Scale bars, 200 μm.

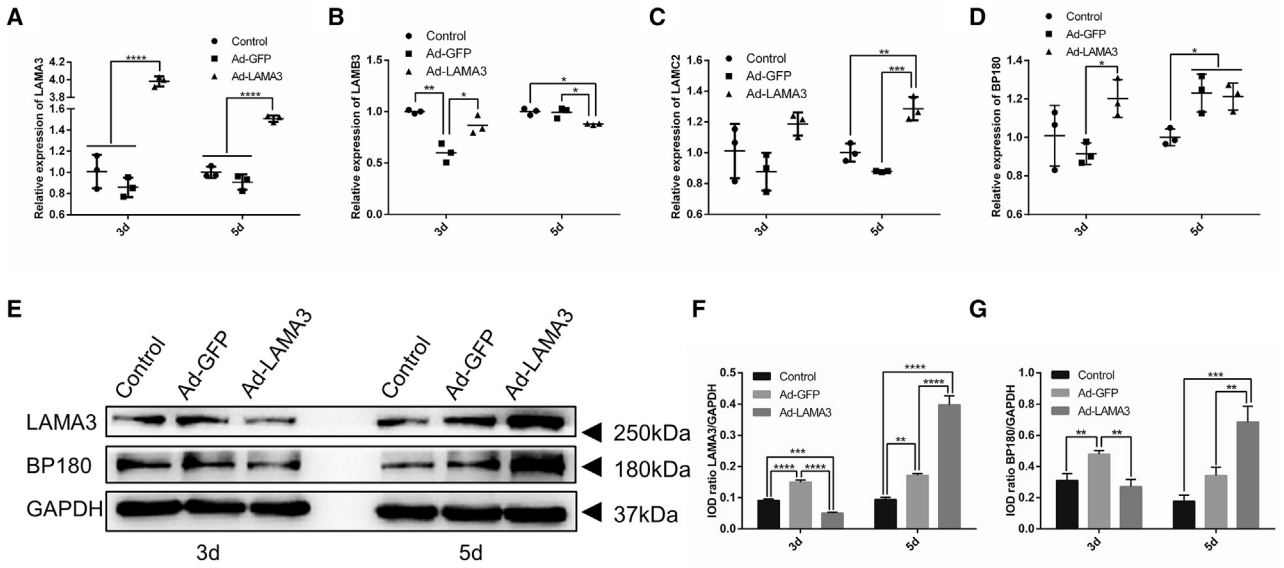

Figure 2. Ad-LAMA3 Facilitates the Expression Levels of HD-Related Gene and Protein

(A–D) Relative mRNA expression of LAMA3 (A), LAMB3 (B), LAMC2 (C), and BP180 (D) 3 or 5 days after transduction with Ad-GFP or Ad-LAMA3. (E) Western blots of HD-related proteins. Expression of LAMA3 and BP180 3 or 5 days after transduction with Ad-GFP or Ad-LAMA3. (F and G) Relative protein expression of LAMA3 (F) and BP180 (G) was normalized to that of GAPDH. Bars represent the mean ± standard deviation for n = 3. *$p < 0.05$, **$p < 0.01$, ***$p < 0.001$, ****$p < 0.0001$.

the JE. 2 days after surgery, the JE was destroyed and separated from the tooth surface in the three groups (Figure 5A). Figure 5B shows efficient expression of the GFP of Ad-GFP and Ad-LAMA3 groups 2 days after injection. The adenovirus showed good transduction into the JE cells. The injured JE "crawled" along with the connective tissue below and proliferated into a long, cord-like structure. 14 days after surgery, the apical portion of the JE of each group was dramatically thicker than that after 7 days, and almost all of it was reattached to the cement–enamel junction. The pathologic morphology of the three groups was not notably different (Figure 5C).

Overexpression of LAMA3 Promotes the Expression of the HD-Related Proteins and HD Formation

Immunohistochemical deposition of BP180 was localized along the tooth–JE interface, JE–connective-tissue interface, and basement membrane in the control group and Ad-LAMA3 group (Figure 6A).

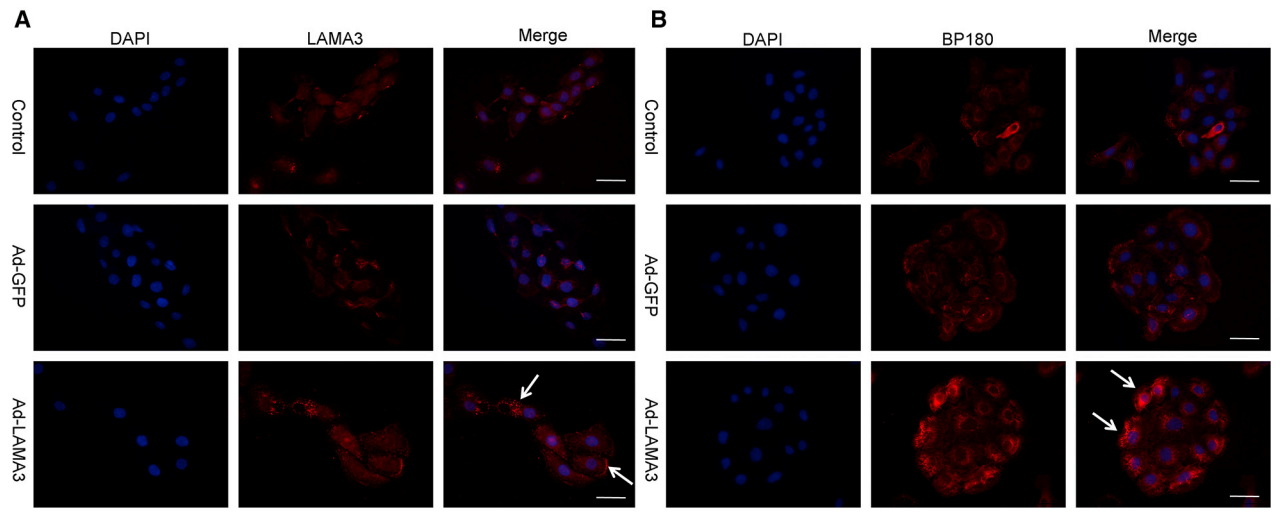

Figure 3. Immunofluorescent Subcellular Localization of LAMA3 and BP180 Proteins in the HaCaT cells

(A and B) Subcellular localization of the LAMA3 proteins (A) and BP180 proteins (B) in HaCaT cells was determined by immunofluorescence microscopy. The merged image shows staining of LAMA3 and BP180, respectively, which were localized in the cytoplasm and cell membrane in the Ad-LAMA3 group (white arrows). Scale bars, 50 μm.

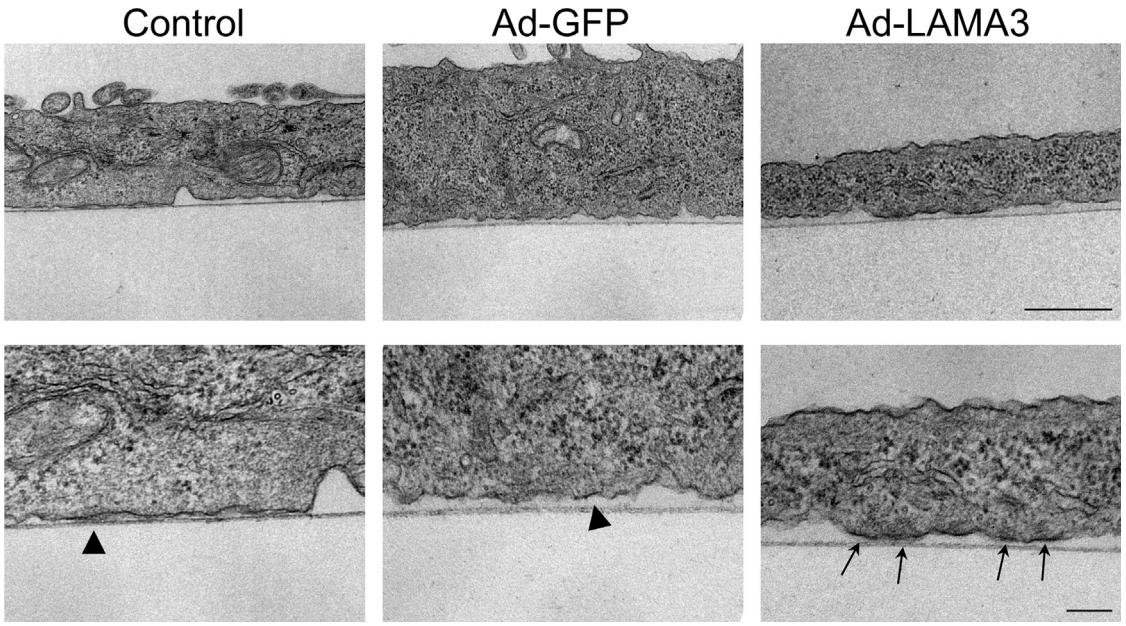

Figure 4. Ad-LAMA3 Promotes Mature HD Formation

Electron micrographs of HaCaT cells grown for 3 days after transduction with Ad-GFP or Ad-LAMA3. In control and Ad-GFP groups, HaCaT cells formed immature pre-HDs (black triangle). In the Ad-LAMA3 group, HaCaT cells formed a group of mature HDs (black arrows). Scale bar, top, 1 μm; bottom, 200 nm.

However, most of the coronal portion of the tooth–JE interface in the saline group and Ad-GFP group did not express BP180. Furthermore, the immunoreaction of LAMA3 was weak in the saline group and Ad-GFP group (Figure 6B).

To evaluate further HD formation along the tooth–JE interface at different times, immunofluorescence double staining for integrin β4 (green) and plectin (red) was done. The integral colocalized linear structure of integrin β4 and plectin in the control group was observed from the coronal to the apical portion of the JE (Figure 7A). 7 days after surgery, the coexpression region appeared mainly in the coronal portion, which was short and discontinuous. However, colocalization staining in the Ad-LAMA3 group was more apparent and longer along the tooth–JE interface than that in the other two groups. 14 days after surgery, the colocalization band increased gradually from the coronal region to the apical region of the JE in all groups. Furthermore, the colocalization band in the LAMA3 group extended to the entire length of the JE, just like in the control group (Figure 7B).

Overexpression of LAMA3 Decreases the Penetration Distance by HRP into the JE after Topical Application

We topically applied horseradish peroxidase (HRP) to the JE to evaluate epithelium sealing during wound healing. Pictures in the four groups showed that 3,3′-diaminobenzidine (DAB)-positive reactions based on endogenous peroxidase were obvious in erythrocytes in capillaries, as well as in neutrophils and macrophages within the JE and connective tissue, which was consistent with the results of a previous study.[25] Stronger and broader HRP reactions were observed from the coronal portion to the apical portion of the JE in the saline and Ad-GFP groups (Figure 8A). In control and Ad-LAMA3 groups, the penetration distance of the HRP reaction was shorter than that in the other two groups ($n = 5$; $p < 0.05$) (Figure 8B). A 1.1-fold decrease in penetration distance at 14 days was observed in the JE transduced with Ad-LAMA3 compared with Ad-GFP.

DISCUSSION

We aimed to evaluate new treatment to induce fast and effective formation of biological closure and stable reattachment of the gingival epithelium. Expression of LAMA3 and BP180 in epithelial cells and HD assembly was documented, and the biological seal between the tooth and gingival epithelium could be improved, using adenovirus-mediated LAMA3 transduction. These actions led to acceleration of HD formation and PR.

The interaction of LM332 and integrin α6β4 enhances epithelial cell adhesion and HD formation.[8,26,27] More research evidence posits that the modification of LAMA3 to the implant surface through a gene-delivery vector promotes the biological sealing of the peri-implant epithelium.[21,28] Presently, we utilized the adenovirus vector to overexpress the LAMA3 gene due to its large size. Future studies should be conducted to identify the most pivotal functional fragment of the LAMA3 gene involved in the formation of HDs.[29,30] In the current study, regarding GFP expression, adenoviral vectors have high transduction efficiency, which reduces the dose of the viral vector and increases therapeutic safety, consistent with the findings of previous studies.[31,32]

To make a biological assessment of Ad-LAMA3 *in vitro*, we selected HaCaT cells. First, the viability of HaCaT cells for Ad-LAMA3

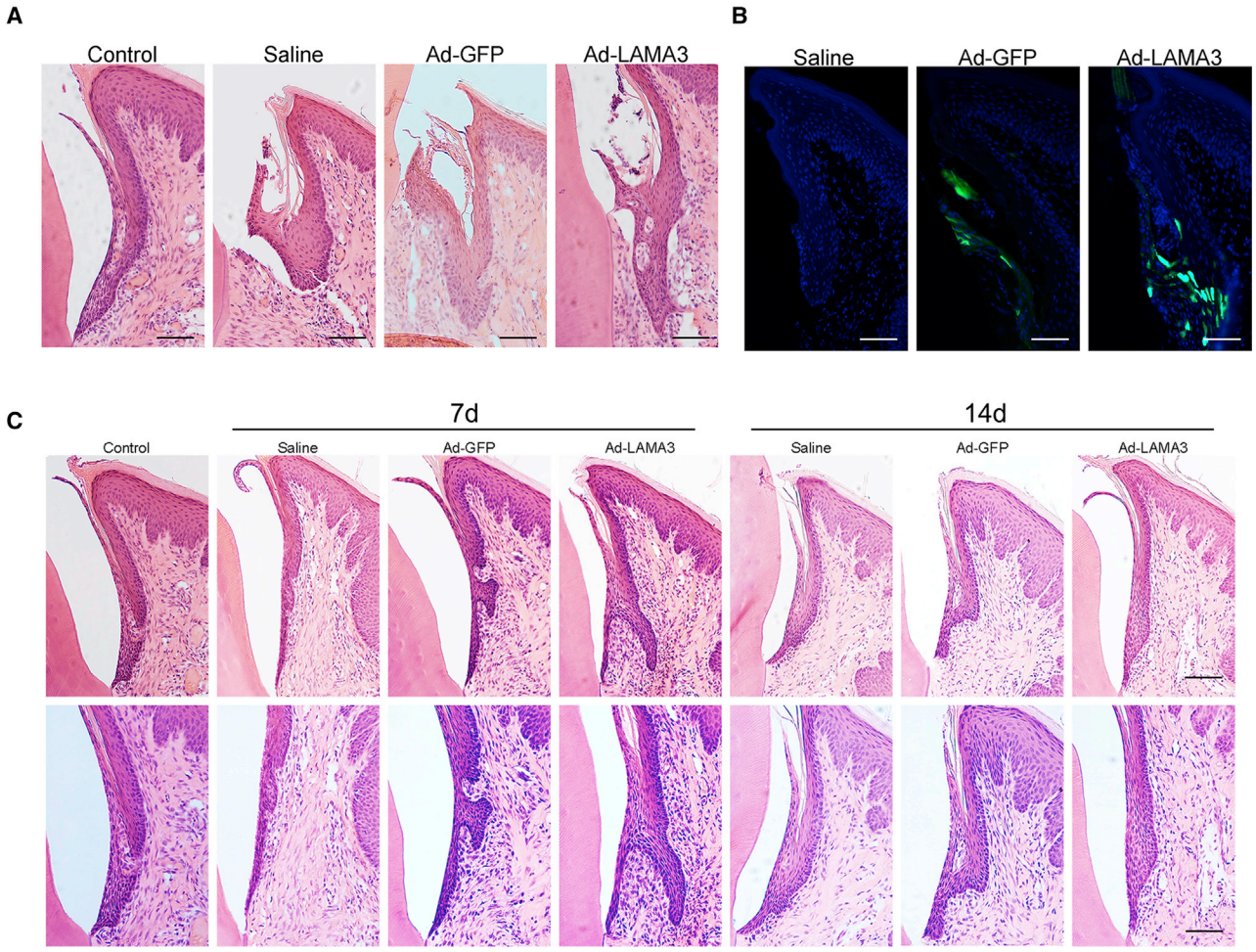

Figure 5. Histology after H&E Staining Demonstrated the JE Healing Process

(A and C) At 2 (A) and 7 and 14 (C) days after injury to the JE. (B) Fluoroscopy shows the effect of adenovirus transduction and expression of green fluorescent protein, 2 days after injection. (A and B) Scale bars, 200 μm. (C) Scale bar, top, 200 μm; bottom, 100 μm.

treatment was evaluated. Consequently, no significant difference at each time point in the three groups was shown. However, a previous investigation indicated that cell viability in the CS/(HA/COL)5-AdLAMA3 group is significantly higher than in the polished titanium group on day 1.[21] This inconsistency could be attributed to the different methods of adenovirus transduction and different interfaces of cell culture. We further evaluated the cell early adhesion, morphology, and migration of HaCaT cells. Representative images and the number of adherent cells indicated that Ad-LAMA3 treatment accelerates cellular attachment, consistent with the findings of a recent study.[28] However, we did not report any significant difference in day 1 in all of the groups regarding the proportion of wound healing. This is because HD depolymerization had not been fully activated.[33–35]

Interestingly, the overexpression of LAMA3 improved the LAMA3 and LAMC2 gene expression, simultaneously and significantly. The LAMC2 gene possesses the unique LM332 chain, which enhances cell adhesion and the formation of HDs.[36] Therefore, from our findings, the expressions of LAMA3 and LAMC2 have synergistic effects. Notably, Ad-LAMA3 therapy showed a pronounced increase in protein expression of LAMA3 and BP180 from 3 days to 5 days, which is consistent with wound healing. Furthermore, the downregulation of protein expression was consistent with the cell-migration results on day 3. Because of the green fluorescence interference of GFP, we did not locate the colocalization HD-like structure *in vitro* using the double-immunofluorescence staining method utilized in our previous study.[21] However, the deposition of LAMA3 and BP180 in the cytoplasm and cell membrane equally indicates HD formation. BP180 is one of the components of HDs. It takes part in adhesion of basal keratinocytes to the extracellular matrix.[37] In addition, appropriate integration of LM332 in the matrix requires BP180, which has a crucial function in the ectodomain to combine LM332 and to regulate the migration and anchorage of

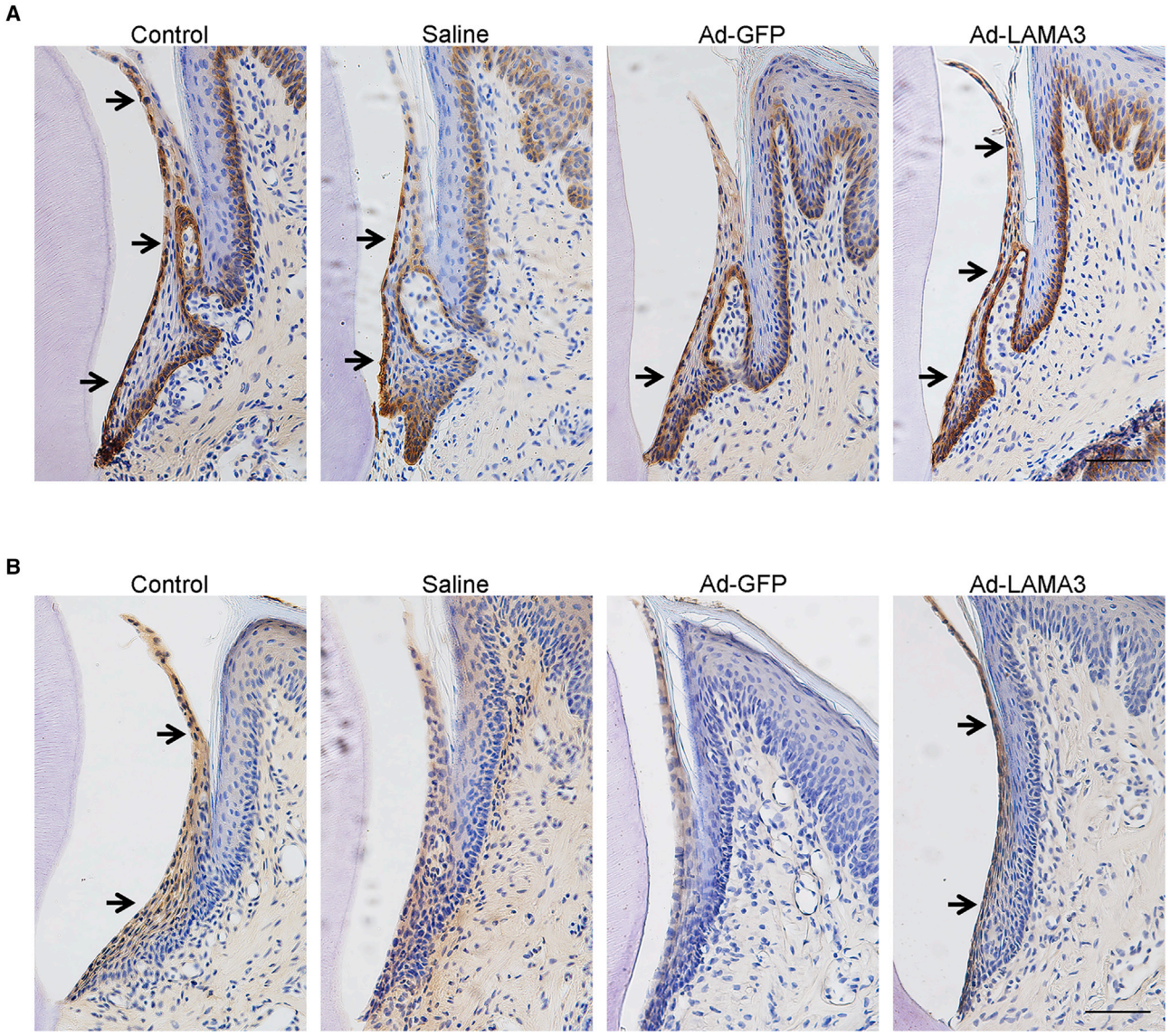

Figure 6. Ad-LAMA3 Enhances the Expression of BP180 and LAMA3 *In Vivo*

(A and B) Immunohistochemical staining indicating expression of BP180 (A) and LAMA3 (B) along the tooth–JE interface 14 days after surgery. Scale bars, 100 μm.

basal keratinocytes.[34,38] Thus, BP180 contributes significantly to HD stabilization. Therefore, the upregulation of expression of these proteins by Ad-LAMA3 during wound healing contributed to HD assembly after migration and integration had been completed, which increased the quantity and quality of HDs in the JE.[39] These actions were further confirmed by TEM data.

Besides *in vitro* experiments, we additionally designed a series of *in vivo* experiments to assess the effect of Ad-LAMA3 on PR. Gene delivery *in vivo* (e.g., intravenous administration) requires high viral doses, as well as provides relatively inefficient transduction in the target cells.[40] In the present study, recombinant LAMA3 adenovirus was transduced efficiently into epithelial cells via local injection, as previously described.[41,42] We established a rat model of JE injury in the first upper molar. To confirm that the apical region of the reattached JE ended at the cement–enamel junction, we used the hematoxylin and eosin (H&E) staining method. Histomorphological results revealed that the long JE was barely formed. However, there was no obvious difference in the morphology of JE among the three groups after wound healing; the fast ability of JE to self-renew may be the most likely explanation for our results.[43,44] The self-renewal time of the normal JE is 1–6 days. Therefore, it is difficult to distinguish them morphologically. Notably, the effect of Ad-LAMA3 treatment in promoting PR was documented using a series of tests,

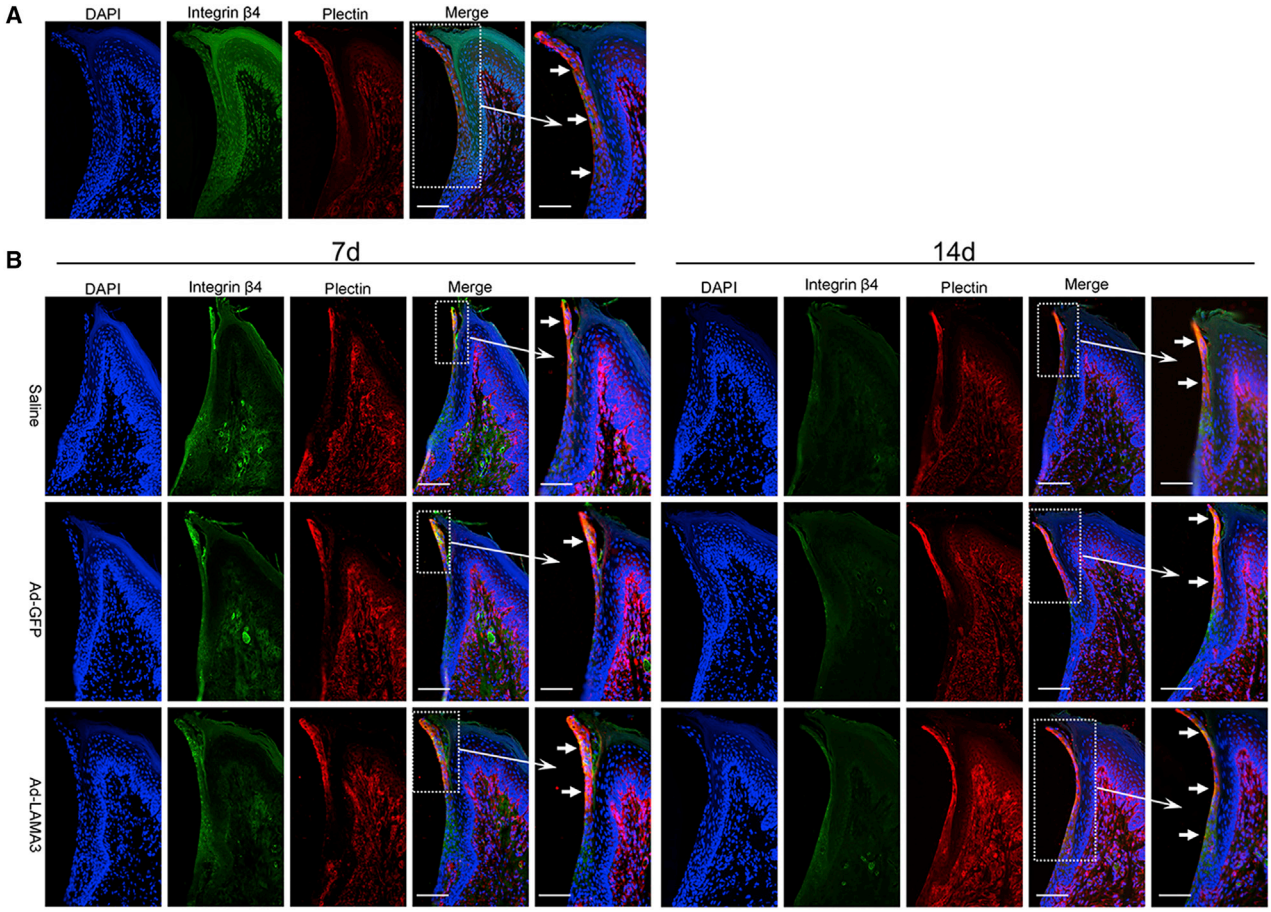

Figure 7. Double-Immunofluorescence Staining Colocalizes HD Formation *In Vivo*

(A) The double-immunofluorescence staining in the normal control group. Scale bar, fourth column, 200 μm; fifth column, 100 μm. (B) Double-immunofluorescence staining, 7 and 14 days after surgery. The integrin β4 (green) colocalizes with plectin (red) in merged images shown as an HD-like structure. Scale bar, fourth and ninth column, 200 μm; fifth and tenth column, 100 μm.

including immunohistochemistry, immunofluorescence double staining, and topical application of HRP.

Consistent with the *in vitro* experiment, we detected the protein expression levels of LAMA3 and BP180 *in vivo*. Our results revealed a strong immunoreactive band along the full length of the tooth–JE interface in the Ad-LAMA3 group, which was consistent with the IBL region.[45,46]

Next, we explored if Ad-LAMA3 promoted HD formation. Scholars have shown that the interaction between integrin β4 and plectin has a crucial role in HD assembly.[33,35,47] Double-fluorescence labeling of integrin β4 and plectin indicated that Ad-LAMA3 could facilitate the assembly and integration of HDs at the whole-tooth–JE interface. However, previous studies have confirmed that HDs only form in the apical and middle portions of the peri-implant epithelium around implants.[48,49] These inconsistent findings could be attributed to the mouse model expressing a truncated form of ameloblastin, resulting in the JE defects.[50] Future studies should be conducted to modify the titanium surface with ameloblastin. Interestingly, our data revealed that the colocalization band, indicating HDs first formed in the coronal region of the JE, since the cells directly attached to the tooth, migrates and adheres toward the crown.[44] To verify the efficacy of epithelial reattachment, we adopted the HRP-penetration assay to assess the biological sealing of the tooth–JE interface.[49] From the penetration distance of the HRP reaction, the Ad-LAMA3 group exhibited higher biological sealing capacity than the saline and Ad-GFP groups. We demonstrated that Ad-LAMA3 could promote and accelerate re-epithelization and reattachment.

Overexpression of human LAMA3 was undertaken using adenoviral vectors, which synthesized LAMA3 effectively *in vitro*. Local transduction by Ad-LAMA3 in a rat model of JE injury promoted the adhesion and migration of epithelial cells and HD formation with upregulation of LAMA3 expression. These actions improved epithelial healing and reattachment. Taken together, these findings suggest that gene therapy,

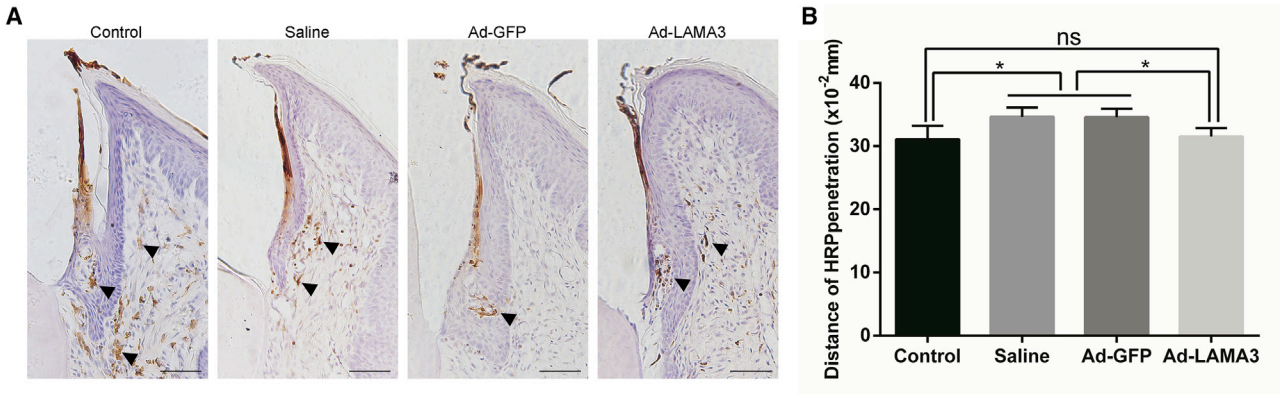

Figure 8. HRP Penetration Evaluates the Biological Sealing of JE

(A) Light micrographs of the JE around the tooth after HRP penetration. The black arrowheads indicate DAB-positive reactions based on endogenous peroxidase. Hematoxylin staining. Original magnification, ×200. Scale bars, 200 μm. (B) Mean distance of HRP penetration. Bars represent the mean ± standard deviation for n = 5. *p < 0.05; ns, p > 0.05.

based on local Ad-LAMA3 transduction, was uncomplicated, practicable, minimally invasive, and relatively inexpensive. In the short term, verification of our data in large studies is needed.

MATERIALS AND METHODS

Adenoviral Vectors, Cell Line, Cell Culture, and Gene Transduction

The LAMA3-overexpressing adenovirus (Ad-LAMA3) and Ad-GFP were constructed by Vigene Biosciences (Shandong, China). The full-length sequence of the LAMA3 gene (accession number National Center for Biotechnology Information [NCBI]: NM_000227) was retrieved from the NCBI database (https://www.ncbi.nlm.nih.gov/gene). The size of the LAMA3 gene is 5,175 bp. The adenovirus vectors were driven using the cytomegalovirus (CMV) promoter (Figure 1A). The titers of Ad-LAMA3 or Ad-GFP were 10^{10} plaque-forming units (PFUs)/mL. HaCaT cells (Xiangf Bio, Shanghai, China) were cultured in Dulbecco's modified Eagle's medium (DMEM; Jima, Beijing, China) with 10% fetal bovine serum (FBS; Gibco, Billings, MT, USA) and 1% penicillin/streptomycin at 37°C in an atmosphere of 5% CO_2. Third-generation cells were used for experiments. HaCaT cells were seeded at 3×10^5 cells/well in six-well dishes. After culturing for 24 h, the cells were transduced with Ad-LAMA3 or Ad-GFP for 12 h, following the manufacturer's instructions, when the cultures reached about 50% confluence, whereas the cells were added to the cell medium alone as a blank control. The medium was changed every 2–3 days, and cells were passaged when cell confluence reached >80%.

Assessment of the Ad-LAMA3 Transduction Efficiency

HaCaT cells were seeded in 24-well plates at 2×10^4 cells/well. After culturing for 24 h, the cells were transduced with the Ad-LAMA3 at different MOIs of 110, 220, or 440 for 48 h. Samples were fixed with 4% paraformaldehyde for 30 min, and nuclei were stained with 4′,6-diamidino-2-phenylindole (DAPI) for 5 min. Then, the transduction efficiency was assessed by calculating the percent of GFP-positive cells under an inverted fluorescence microscope (AXIO Observer A1; Zeiss, Wetzlar, Germany). The number of GFP-positive cells in three randomly selected fluorescent pictures was counted using ImageJ (National Institutes of Health, Bethesda, MD, USA) to demonstrate the transduction efficiency.

Proliferation Assay

The viability of HaCaT cells was evaluated by the alamarBlue test. HaCaT cells were seeded in 12-well plates at 2×10^4 cells/well. After transduction for 1, 3, or 5 days, the medium was replaced with a medium containing 10% alamarBlue cell viability reagent (Invitrogen, Carlsbad, CA, USA) at 37°C in a 5% CO_2 incubator with the atmosphere humidified for 4 h. Changes in light intensity of the incubation solution (100 μL) were measured by a microplate spectrophotometer (Spectra M2; Molecular Devices, Silicon Valley, CA, USA) at an excitation wavelength of 540 nm and emission wavelength of 590 nm. Each group contained three wells, and the mean value served as the final result.

Adhesion Assay in Early Stages

The transduced HaCaT cells were seeded in 24-well plates at 2×10^4 cells/well and cultured for 3 h or 6 h. Samples were washed with ice-cold phosphate-buffered saline (PBS) and then fixed in 4% paraformaldehyde at room temperature for 30 min. Then, the cells were permeabilized in 0.5% Triton X-100 (Solarbio, Beijing, China) for 5 min. The cytoskeleton was stained using tetra-methyl-5,6-isothiocyanate-phalloidin (Solarbio) in the dark for 30 min at room temperature. Nuclei were stained with DAPI for 5 min. Samples were washed thrice with PBS at each step. The cell morphology and cytoskeleton were analyzed using a Nikon A1 confocal laser-scanning microscope (CLSM; Nikon, Tokyo, Japan). Cell numbers were counted at three sites, chosen randomly on each group, using ImageJ (National Institutes of Health, Bethesda, MD, USA).

Scratch Assays

Scratch assays were carried out as wound models on dishes. In a confluent monolayer of HaCaT cells after adenovirus infection, a

scratch was made with 200 μL pipette tips. The width of the scratch was measured at the beginning, as well as after 1 day or 3 days, of culture in DMEM with 1% FBS. The percent of wound closure was calculated using ImageJ.

Western Blotting

After 3 days or 5 days of cell culture, samples were washed with ice-cold PBS. Then, the total protein was extracted by lysing in radioimmunoprecipitation assay (RIPA) buffer with a "cocktail" of protease inhibitors (Beyotime Biotechnology, Beijing, China). The three groups of cell lysates were quantified using a bicinchoninic acid protein kit (ComWin Biotech, Beijing, China). About 20 μg of protein was separated by sodium dodecyl sulfate-polyacrylamide gel electrophoresis using 8% gels (Invitrogen). Proteins were transferred onto polyvinylidene fluoride (PVDF) membranes (Millipore, Bedford, MA, USA) for immunoblotting and then blocked with 5% skimmed milk in Tris-buffered saline-Tween 20 (TBST) buffer for 2 h at room temperature. PVDF membranes were incubated with primary antibodies against rabbit LAMA3 (Abcam, Cambridge, UK), mouse integrin β4 (Abcam), and glyceraldehyde 3-phosphate dehydrogenase (GAPDH; Bioker, Beijing, China) overnight at 4°C. PVDF membranes were rinsed with TBST and then incubated with the corresponding secondary antibody (immunoglobulin G [IgG]-HRP; Bioker) for 1 h at room temperature. Antibody-bound bands were visualized using an enhanced chemiluminescence system (Millipore), and the gray value of each band was measured with ImageJ.

Quantitative Real-Time Polymerase Chain Reaction

After 3 days or 5 days of cell culture, total RNA was extracted from HaCaT cells using TRIzol reagent (Invitrogen). Complimentary DNA (cDNA) was synthesized using a PrimeScript RT Reagent kit (Perfect Real Time; TaKaRa Biotechnology, Dalian, China). Quantitative real-time PCR was done using a SYBR Green kit (TaKaRa Biotechnology) with an ABI ViiA 7 system (Applied Biosystems, Foster City, CA, USA). The PCR conditions were the following: initial denaturation at 95°C for 30 s, followed by denaturation at 95°C for 5 s and annealing at 60°C for 34 s for 40 cycles. The relative expression of genes from three independent experiments was analyzed using the $2^{-\rho\rho CT}$ method. All CT values were averaged and calibrated by the CT value of GAPDH. The sequences of the primers were as follows: LAMA3 (NCBI: NM_000227), 5′-CTGCAGTTTAAACAAACCACCT-3′ (forward) and 5′-CAGCTGGTTGATACGAAAAGTC-3′ (reverse); LAMB3 (NCBI: NM_000228), 5′-GAGCCTGTGACTGTGATTTCC-3′ (forward) and 5′-GGTAGCGATTACAGTAGCCTC-3′ (reverse); LAMC2 (NCBI: NM_005562), 5′-GAGGATCAAACAAAAAGCG GAT-3′ (forward) and 5′-AGATTCTTCTGTGTACGCTTGA-3′ (reverse); BP180, 5′-TCGTCTTACTTACATACTGCCG-3′ (forward) and 5′-CTG TTTTCAGCTGCATAGGTTG-3′ (reverse); and GAPDH, 5′-GCACCGTCAAGGCTGAGAAC-3′ (forward) and 5′-TGGTGAAGACGCCAGTGGA-3′ (reverse).

Immunofluorescence Assay

HaCaT cells were seeded at 2×10^4 cells/well onto glass slides (macrophage = 20 mm) in 12-well plates. 2 days after transduction, samples were fixed with 4% paraformaldehyde for 30 min and permeabilized in 0.5% Triton X-100 for 5 min. Samples were blocked with 2% bovine serum albumin for 30 min. Then, HaCaT cells were incubated overnight at 4°C with rabbit primary antibodies against anti-LAMA3 (1:100 dilution; Abcam) or anti-BP180 (1:100; Abcam). All samples were incubated with a Cy3-conjugated anti-rabbit secondary antibody (1:100 dilution; Proteintech, Beijing, China) for 1 h at room temperature. Nuclei were stained with DAPI. Samples were washed thrice with PBS at each step, except for blockade. Fluorescence micrographs were taken using an upright fluorescence microscope (DM4000; Leica). Images were captured using a Leica DFC450 C camera.

TEM

The protocols for TEM were similar to that described by Jones and colleagues.[51] Briefly, HaCaT cells were seeded at 30×10^4 cells/well onto glass slides (macrophage = 24 mm) in six-well plates. 3 days after transduction, samples were fixed in 2.5% glutaraldehyde (pH 7.4) at 4°C overnight and then washed thrice in 0.1 M PBS. Then, HaCaT cells were fixed in 1% osmium tetroxide for 1 h at room temperature and washed thrice with 0.1 M PBS. Samples were stained in 2% uranyl acetate for 1 h. Samples were dehydrated through a graded series of ethanol solutions up to 100% and infiltrated in Spurr resin. The following day, samples were embedded in inverted Eppendorf tubes containing Spurr resin and heated at 60°C for 48 h. Samples were sectioned in an electron microscopy (EM) UC7 ultratome (Leica). Sections were stained with uranyl acetate and alkaline lead citrate for 5–10 min, respectively, and examined using a transmission electron microscope (TECNAI-10; Philips, Netherlands).

Animal Model

The study protocol was approved by the Ethics Committee of Zhejiang University (Hangzhou, China). Forty-two male Wistar rats (180–220 g) were divided randomly into three groups of 12 (Ad-LAMA3, Ad-GFP, and saline) and one group of six (normal control). Briefly, rats were anesthetized with 10% chloral hydrate (0.3 mL/100 g bodyweight, intraperitoneally [i.p.]). A sterile periodontal probe was placed parallel to the tooth surface, along with the first molar buccal sulcus on both sides of the maxilla. JE tissues of 36 rats were injured by continuous multiple-point puncture by lifting and insertion around the tooth, with the depth maintained to the top of the alveolar ridge. After hemostasis, 5 μL of Ad-LAMA3, Ad-GFP, or physiologic (0.9%) saline was injected into the buccal sulcus using a microliter syringe (Gaoge, Shanghai, China). After injection, the rats were allowed to have standard chow and tap water *ad libitum* under conventional laboratory conditions.

Tissue Preparation

At 2, 7, and 14 days after surgery, deep anesthesia was induced. This was followed by transcardial perfusion of heparinized saline. Next, cold fixative containing 4% paraformaldehyde (pH 7.4) was administered. Bilateral maxillae were dissected immediately after perfusion and immersed in the same fixative for 4 h at 4°C and then demineralized in 0.5 M EDTA solution for 2 weeks at room temperature.

Tissue samples were maintained in 0.01 M PBS containing 20% sucrose for cryoprotection. Then, specimens were embedded in optimal cutting temperature compound (Sakura, Tokyo, Japan) and stored at −80°C until cryosection. After being balanced at −20°C, gingiva samples were cut bucco palatally into 10 μm-thick cryosections. Cryosections were mounted on adhesion microscope slides (Servicebio, Wuhan, China).

Staining Using H&E and DAPI

After rinsing with 0.01 M PBS, cryosections, 2, 7, and 14 days after surgery, were stained with H&E. To observe the transduction efficiency of adenoviruses *in vivo*, 2 days after surgery cryosections were washed in 0.01 M PBS and stained with DAPI. Slices were observed under a light microscope and fluorescence microscope.

Immunohistochemistry

Instant Immunohistochemistry Kit I (for application on rabbit primary antibodies) (Dako, Glostrup, Denmark) was used. Briefly, after tissue sections had been washed in 0.01 M PBS, tissue sections were treated with 3% H_2O_2 in PBS for 10 min and blocked for 30 min with 10% normal goat serum in PBS. Then, tissue sections were incubated overnight at 4°C with primary rabbit polyclonal anti-LAMA3 antibody (1:100 dilution; Bioss, Beijing, China) and BP180 (1:100; Abcam). Tissue sections were incubated with HRP-labeled secondary antibody (goat anti-rabbit) in PBS (1:200 dilution) for 30 min at room temperature. Then, tissue sections were treated in DAB for 5 min. All tissue sections were washed in PBS and counterstained with hematoxylin. Tissue sections were examined and photographed under a light microscope.

Immunofluorescence Double Staining

According to the method described by Zhang et al.,[21] the colocalization of integrin β4 and plectin was used to indicate the structure of HDs. Briefly, samples were incubated overnight with a solution containing anti-integrin β4 mouse monoclonal antibody and anti-plectin rabbit monoclonal antibody at 4°C. Then, sections were incubated with two secondary antibodies: goat anti-mouse IgG conjugated with Alexa 488 and goat anti-rabbit IgG conjugated with Cy3. Nuclei were stained with DAPI. Sections were photographed using a fluorescence microscope.

Topical Application of HRP

14 days after surgery, 50 mg/mL of HRP (40,000 Da; Solarbio) was applied topically to 12 rats (three rats in each group). The procedure for topical application of HRP was similar to that reported by Atsuta and et al.[52] Briefly, under general anesthesia, cotton floss immersed in 10 μL of HRP/PBS (50 mg/mL) was laid on the gingival margin around the tooth without application of mechanical stress. Then, the same volume of solution was dripped onto the floss every 10 min for 60 min. Preparation of gingival sections was done as described above. After sections had been washed in PBS, they were incubated in a DAB substrate kit (Solarbio) for 5 min at room temperature. All sections were counterstained with hematoxylin. Five sections from each group were selected. The vertical distance between the top of the JE and the bottom of the area where HRP had penetrated was measured parallel to the long axis of the tooth.

Statistical Analyses

Independent experiments were carried out using triplicate samples and were repeated at least thrice. Statistical analyses were carried out using SPSS v22.0 (IBM, Armonk, NY, USA). One-way analysis of variance with Fisher's least significant difference test was used to analyze differences in multiple comparisons with all groups. Data are the mean ± standard deviation. $p < 0.05$ was considered significant.

AUTHOR CONTRIBUTIONS

Y.L., J.Z., and K.L. designed the experiments. Y.L., X.D., Z.C., and T.H. carried out the experiments. Y.W., Z.J., and G.Y. analyzed the data. Y.L., J.Z., K.L., and G.Y. drafted and revised the manuscript. All authors read and approved the submitted manuscript.

CONFLICTS OF INTEREST

The authors declare no competing interests.

ACKNOWLEDGMENTS

We thank Beibei Wang in the Center of Cryo-Electron Microscopy (CCEM), Zhejiang University, for her technical assistance on transmission electron microscopy. This work was supported by the National Natural Science Foundation of China (grant numbers 81801026 and 81701021).

REFERENCES

1. Gibbs, S., Roffel, S., Meyer, M., and Gasser, A. (2019). Biology of soft tissue repair: gingival epithelium in wound healing and attachment to the tooth and abutment surface. Eur. Cell. Mater. *38*, 63–78.

2. Puvvalla, B., Suchetha, A., Mundinamanae, D.B., Apoorva, S.M., and Bhat, D. (2018). Unfolding Various Concepts of Junctional Epithelium. J. Health Allied Sci. NU *8*, 35–44.

3. Isidor, F., Karring, T., Nyman, S., and Lindhe, J. (1985). New attachment-reattachment following reconstructive periodontal surgery. J. Clin. Periodontol. *12*, 728–735.

4. Giannobile, W.V. (2008). Host-response therapeutics for periodontal diseases. J. Periodontol. *79* (8, Suppl), 1592–1600.

5. Hormia, M., Owaribe, K., and Virtanen, I. (2001). The dento-epithelial junction: cell adhesion by type I hemidesmosomes in the absence of a true basal lamina. J. Periodontol. *72*, 788–797.

6. Sawada, T., Yamazaki, T., Shibayama, K., Kumazawa, K., Yamaguchi, Y., and Ohshima, M. (2014). Expression and localization of laminin 5, laminin 10, type IV collagen, and amelotin in adult murine gingiva. J. Mol. Histol. *45*, 293–302.

7. Schneider, H., Mühle, C., and Pacho, F. (2007). Biological function of laminin-5 and pathogenic impact of its deficiency. Eur. J. Cell Biol. *86*, 701–717.

8. Baker, S.E., Hopkinson, S.B., Fitchmun, M., Andreason, G.L., Frasier, F., Plopper, G., Quaranta, V., and Jones, J.C.R. (1996). Laminin-5 and hemidesmosomes: role of the α 3 chain subunit in hemidesmosome stability and assembly. J. Cell Sci. *109*, 2509–2520.

9. Goldfinger, L.E., Hopkinson, S.B., deHart, G.W., Collawn, S., Couchman, J.R., and Jones, J.C. (1999). The alpha3 laminin subunit, alpha6beta4 and alpha3beta1 integrin coordinately regulate wound healing in cultured epithelial cells and in the skin. J. Cell Sci. *112*, 2615–2629.

10. Goldfinger, L.E., Jiang, L., Hopkinson, S.B., Stack, M.S., and Jones, J.C. (2000). Spatial regulation and activity modulation of plasmin by high affinity binding to the G domain of the alpha 3 subunit of laminin-5. J. Biol. Chem. *275*, 34887–34893.

11. Yamashita, H., Tripathi, M., Harris, M.P., Liu, S., Weidow, B., Zent, R., and Quaranta, V. (2010). The role of a recombinant fragment of laminin-332 in integrin alpha3-beta1-dependent cell binding, spreading and migration. Biomaterials *31*, 5110–5121.

12. Vidal, F., Baudoin, C., Miquel, C., Galliano, M.F., Christiano, A.M., Uitto, J., Ortonne, J.P., and Meneguzzi, G. (1995). Cloning of the laminin alpha 3 chain gene (LAMA3) and identification of a homozygous deletion in a patient with Herlitz junctional epidermolysis bullosa. Genomics *30*, 273–280.

13. Gostyńska, K.B., Yan Yuen, W., Pasmooij, A.M., Stellingsma, C., Pas, H.H., Lemmink, H., and Jonkman, M.F. (2016). Carriers with functional null mutations in LAMA3 have localized enamel abnormalities due to haploinsufficiency. Eur. J. Hum. Genet. *25*, 94–99.

14. Kim, J.M., Park, W.H., and Min, B.M. (2005). The PPFLMLLKGSTR motif in globular domain 3 of the human laminin-5 alpha3 chain is crucial for integrin alpha3-beta1 binding and cell adhesion. Exp. Cell Res. *304*, 317–327.

15. Abdallah, M.N., Badran, Z., Ciobanu, O., Hamdan, N., and Tamimi, F. (2017). Strategies for Optimizing the Soft Tissue Seal around Osseointegrated Implants. Adv. Healthc. Mater. *6*, 1700549.

16. Koidou, V.P., Argyris, P.P., Skoe, E.P., Mota Siqueira, J., Chen, X., Zhang, L., Hinrichs, J.E., Costalonga, M., and Aparicio, C. (2018). Peptide coatings enhance keratinocyte attachment towards improving the peri-implant mucosal seal. Biomater. Sci. *6*, 1936–1945.

17. Liu, Z.H., Ma, S.Q., Lu, X., Zhang, T., Sun, Y.C., Feng, W., Zheng, G.Y., Sui, L., Wu, X.D., Zhang, X., et al. (2019). Reinforcement of epithelial sealing around titanium dental implants by chimeric peptides. Chem. Eng. J. *356*, 117–129.

18. Werner, S., Huck, O., Frisch, B., Vautier, D., Elkaim, R., Voegel, J.C., Brunel, G., and Tenenbaum, H. (2009). The effect of microstructured surfaces and laminin-derived peptide coatings on soft tissue interactions with titanium dental implants. Biomaterials *30*, 2291–2301.

19. Kanzaki, H., Chiba, M., Arai, K., Takahashi, I., Haruyama, N., Nishimura, M., and Mitani, H. (2006). Local RANKL gene transfer to the periodontal tissue accelerates orthodontic tooth movement. Gene Ther. *13*, 678–685.

20. Tang, H., Mattheos, N., Yao, Y., Jia, Y., Ma, L., and Gong, P. (2015). In vivo osteoprotegerin gene therapy preventing bone loss induced by periodontitis. J. Periodontal Res. *50*, 434–443.

21. Zhang, J., Wang, H., Wang, Y., Dong, W., Jiang, Z., and Yang, G. (2018). Substrate-mediated gene transduction of LAMA3 for promoting biological sealing between titanium surface and gingival epithelium. Colloids Surf. B Biointerfaces *161*, 314–323.

22. Hiroyasu, S., Ozawa, T., Kobayashi, H., Ishii, M., Aoyama, Y., Kitajima, Y., Hashimoto, T., Jones, J.C., and Tsuruta, D. (2013). Bullous pemphigoid IgG induces BP180 internalization via a macropinocytic pathway. Am. J. Pathol. *182*, 828–840.

23. Borradori, L., and Sonnenberg, A. (1999). Structure and function of hemidesmosomes: more than simple adhesion complexes. J. Invest. Dermatol. *112*, 411–418.

24. Hormia, M., Falk-Marzillier, J., Plopper, G., Tamura, R.N., Jones, J.C., and Quaranta, V. (1995). Rapid spreading and mature hemidesmosome formation in HaCaT keratinocytes induced by incubation with soluble laminin-5r. J. Invest. Dermatol. *105*, 557–561.

25. Ikeda, H., Shiraiwa, M., Yamaza, T., Yoshinari, M., Kido, M.A., Ayukawa, Y., Inoue, T., Koyano, K., and Tanaka, T. (2002). Difference in penetration of horseradish peroxidase tracer as a foreign substance into the peri-implant or junctional epithelium of rat gingivae. Clin. Oral Implants Res. *13*, 243–251.

26. Niessen, C.M., Hogervorst, F., Jaspars, L.H., de Melker, A.A., Delwel, G.O., Hulsman, E.H.M., Kuikman, I., and Sonnenberg, A. (1994). The α 6 β 4 integrin is a receptor for both laminin and kalinin. Exp. Cell Res. *211*, 360–367.

27. Sugisawa, M., Masaoka, T., Enokiya, Y., Muramatsu, T., Hashimoto, S., Yamada, S., and Shimono, M. (2010). Expression and function of laminin and integrins on adhesion/migration of primary culture cells derived from rat oral epithelium. J. Periodontal Res. *45*, 284–291.

28. Wang, J., He, X.T., Xu, X.Y., Yin, Y., Li, X., Bi, C.S., Hong, Y.L., and Chen, F.M. (2019). Surface modification via plasmid-mediated pLAMA3-CM gene transfection promotes the attachment of gingival epithelial cells to titanium sheets in vitro and improves biological sealing at the transmucosal sites of titanium implants in vivo. J. Mater. Chem. B Mater. Biol. Med. *7*, 7415–7427.

29. Tsubota, Y., Yasuda, C., Kariya, Y., Ogawa, T., Hirosaki, T., Mizushima, H., and Miyazaki, K. (2005). Regulation of biological activity and matrix assembly of laminin-5 by COOH-terminal, LG4-5 domain of alpha3 chain. J. Biol. Chem. *280*, 14370–14377.

30. Di Zenzo, G., El Hachem, M., Diociaiuti, A., Boldrini, R., Calabresi, V., Cianfarani, F., Fortugno, P., Piccinni, E., Zambruno, G., and Castiglia, D. (2014). A truncating mutation in the laminin-332α chain highlights the role of the LG45 proteolytic domain in regulating keratinocyte adhesion and migration. Br. J. Dermatol. *170*, 1056–1064.

31. Kallel, H., and Kamen, A.A. (2015). Large-scale adenovirus and poxvirus-vectored vaccine manufacturing to enable clinical trials. Biotechnol. J. *10*, 741–747.

32. Xu, M., Tang, X., Guo, J., Sun, W., and Tang, F. (2017). Reversal effect of adenovirus-mediated human interleukin 24 transfection on the cisplatin resistance of A549/DDP lung cancer cells. Oncol. Rep. *38*, 2843–2851.

33. Margadant, C., Frijns, E., Wilhelmsen, K., and Sonnenberg, A. (2008). Regulation of hemidesmosome disassembly by growth factor receptors. Curr. Opin. Cell Biol. *20*, 589–596.

34. Tsuruta, D., Hashimoto, T., Hamill, K.J., and Jones, J.C. (2011). Hemidesmosomes and focal contact proteins: functions and cross-talk in keratinocytes, bullous diseases and wound healing. J. Dermatol. Sci. *62*, 1–7.

35. Litjens, S.H., de Pereda, J.M., and Sonnenberg, A. (2006). Current insights into the formation and breakdown of hemidesmosomes. Trends Cell Biol. *16*, 376–383.

36. Yang, G., Zhang, J., Dong, W., Liu, L., Shi, J., and Wang, H. (2016). Fabrication, characterization, and biological assessment of multilayer laminin γ2 DNA coatings on titanium surfaces. Sci. Rep. *6*, 23423.

37. Walko, G., Castañón, M.J., and Wiche, G. (2015). Molecular architecture and function of the hemidesmosome. Cell Tissue Res. *360*, 529–544.

38. Tasanen, K., Tunggal, L., Chometon, G., Bruckner-Tuderman, L., and Aumailley, M. (2004). Keratinocytes from patients lacking collagen XVII display a migratory phenotype. Am. J. Pathol. *164*, 2027–2038.

39. Iorio, V., Troughton, L.D., and Hamill, K.J. (2015). Laminins: Roles and Utility in Wound Repair. Adv. Wound Care (New Rochelle) *4*, 250–263.

40. Challis, R.C., Ravindra Kumar, S., Chan, K.Y., Challis, C., Beadle, K., Jang, M.J., Kim, H.M., Rajendran, P.S., Tompkins, J.D., Shivkumar, K., et al. (2019). Systemic AAV vectors for widespread and targeted gene delivery in rodents. Nat. Protoc. *14*, 379–414.

41. Tarkka, T., Sipola, A., Jämsä, T., Soini, Y., Ylä-Herttuala, S., Tuukkanen, J., and Hautala, T. (2003). Adenoviral VEGF-A gene transfer induces angiogenesis and promotes bone formation in healing osseous tissues. J. Gene Med. *5*, 560–566.

42. Hu, W.W., Wang, Z., Hollister, S.J., and Krebsbach, P.H. (2007). Localized viral vector delivery to enhance in situ regenerative gene therapy. Gene Ther. *14*, 891–901.

43. Kinumatsu, T., Hashimoto, S., Muramatsu, T., Sasaki, H., Jung, H.S., Yamada, S., and Shimono, M. (2009). Involvement of laminin and integrins in adhesion and migration of junctional epithelium cells. J. Periodontal Res. *44*, 13–20.

44. Yajima-Himuro, S., Oshima, M., Yamamoto, G., Ogawa, M., Furuya, M., Tanaka, J., Nishii, K., Mishima, K., Tachikawa, T., Tsuji, T., and Yamamoto, M. (2014). The junctional epithelium originates from the odontogenic epithelium of an erupted tooth. Sci. Rep. *4*, 4867.

45. Mullen, L.M., Richards, D.W., and Quaranta, V. (1999). Evidence that laminin-5 is a component of the tooth surface internal basal lamina, supporting epithelial cell adhesion. J. Periodontal Res. *34*, 16–24.

46. Sawada, T., Yamazaki, T., Shibayama, K., Yamaguchi, Y., and Ohshima, M. (2015). Ultrastructural immunolocalization of laminin 332 (laminin 5) at dento-gingival interface in Macaca fuscata monkey. Med. Mol. Morphol. *48*, 104–111.

47. Koster, J., van Wilpe, S., Kuikman, I., Litjens, S.H., and Sonnenberg, A. (2004). Role of binding of plectin to the integrin beta4 subunit in the assembly of hemidesmosomes. Mol. Biol. Cell *15*, 1211–1223.

48. Atsuta, I., Ayukawa, Y., Kondo, R., Oshiro, W., Matsuura, Y., Furuhashi, A., Tsukiyama, Y., and Koyano, K. (2016). Soft tissue sealing around dental implants based on histological interpretation. J. Prosthodont. Res. *60*, 3–11.

49. Atsuta, I., Ayukawa, Y., Furuhashi, A., Narimatsu, I., Kondo, R., Oshiro, W., and Koyano, K. (2019). Epithelial sealing effectiveness against titanium or zirconia implants surface. J. Biomed. Mater. Res. A *107*, 1379–1385.

50. Wazen, R.M., Moffatt, P., Zalzal, S.F., Yamada, Y., and Nanci, A. (2009). A mouse model expressing a truncated form of ameloblastin exhibits dental and junctional epithelium defects. Matrix Biol. *28*, 292–303.

51. Riddelle, K.S., Green, K.J., and Jones, J.C.R. (1991). Formation of hemidesmosomes in vitro by a transformed rat bladder cell line. J. Cell Biol. *112*, 159–168.

52. Atsuta, I., Ayukawa, Y., Ogino, Y., Moriyama, Y., Jinno, Y., and Koyano, K. (2012). Evaluations of epithelial sealing and peri-implant epithelial down-growth around "step-type" implants. Clin. Oral Implants Res. *23*, 459–466.